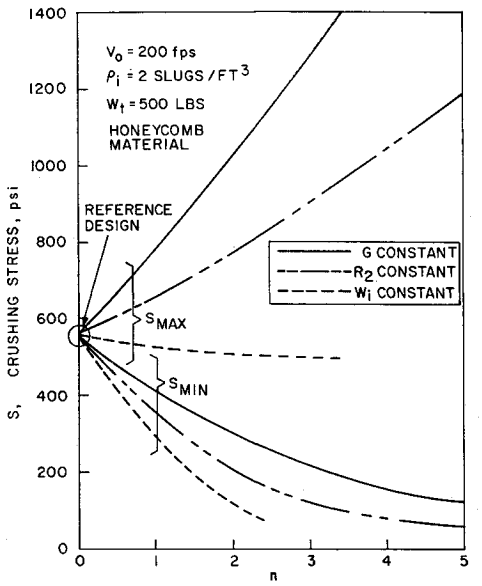


**Fig. 5 Graph of maximum and minimum crushing stress vs degree of nonhomogeneity.**

relating velocity, acceleration, and stroke:

$$v_0^2/\epsilon\ddot{y}_m = 2R_2[1 - u_m - (1 - u_m{}^{n+3})/(n + 3)]/(1 - u_m{}^{n+2}) \quad (8)$$

Now, assuming that the lander is a complete sphere, the mass of the crushable material can be calculated. The incremental mass of a spherical shell of thickness $dR$ is

$$dm_c = 4\pi\rho_c R^2 dR$$

If a single type of crushable material is used, such as aluminum honeycomb, it is possible to fit a curve to the plot of material properties. It has been found, in fact, that a curve of the form $\rho_c = S^\beta/\alpha$ can be fit to most of the materials of interest.[2] Using this equation, the total crush-up mass is

$$m_c = 4\pi\rho_{cm}R_2{}^3(1 - u_m{}^{\beta n+3})/(\beta n + 3) \quad (9)$$

where $\rho_{cm}$ is the mass density corresponding to the maximum crushing stress $S_m$. Equations (7–9), together with an equation for payload mass,

$$m_i = \tfrac{4}{3}\pi\rho_i R_1{}^3 = \tfrac{4}{3}\pi\rho_i R_2{}^3 u_m{}^3 \quad (10)$$

form the basis for parametric studies of the effect of using nonhomogeneous design of crushable-material impact absorbers.

### Example and Conclusions

An impact velocity of 200 fps, a payload packing density of 2 slug/ft$^3$, and a total landed weight of 500 lb are assumed. A honeycomb class of crushable material (either plastic or metal) is specified, for which $\rho_c = S^{0.554}/2080$, and $\epsilon = 0.75$. The reference design is a 1500-$g$ impact with homogeneous material. The results of parametric studies using a digital computer program of the foregoing equations are summarized in Figs. 3–5.

If the deceleration level is held constant at 1500 $g$'s, then increasing $n$ brings about some increase in payload $w_i$ and a significant reduction in outside radius $R_2$. Although the range of crushing stress is quite wide (Fig. 5) the values are achievable with current materials. If, instead, $w_i$ is held fixed while $n$ is increased, a substantial reduction in the $g$ level results, but $R_2$ increases significantly because more ow-density, inefficient honeycomb material is being used. Reference 1 indicates, that for this case using balsa wood, here is little change in $R_2$.) Further, the minimum crushing tress required rapidly decreases to a point where it is unfeasible. A compromise between these two cases can be obtained by holding $R_2$ fixed; then $G$ decreases, $w_i$ increases, and the variations required in $S$ are moderate.

The main problem in implementing this technique would be avoiding the "cannon-ball" effect, where the payload starts to move independently and to crush the energy-absorption material internally.[1,2] If tension ties between the payload and the crushable material are sufficiently strong to prevent this effect, then this technique would allow significant improvements in the design of hard-landing, omnidirectionally protected planetary probes.

### References

[1] Cundall, D. R., "Balsa-wood impact limiters for hard landing on the surface of Mars," *AIAA/AAS Stepping Stones to Mars Meeting* (American Institute of Aeronautics and Astronautics, New York, 1966), pp. 302–308.

[2] Cloutier, G. J., "Landing impact energy absorption using anisotropic crushable materials," J. Spacecraft Rockets **3**, 1755–1761 (1966).

# Potential of Low-Power Thermionic Devices for Terrestrial Applications

F. T. Princiotta* and T. S. Bustard†
*Hittman Associates Inc., Baltimore, Md.*

To date, the bulk of thermionic systems development effort has been related to space utilization. At a lower level of effort has been terrestrial thermionic development, and almost all of this has related to design of hydrocarbon-fired thermionic devices. Only a very small effort has been expended on development of isotope-fueled terrestrial thermionic generators. This note presents an evaluation of the potential of such nuclear systems.

The main development problem associated with hydrocarbon-fired generators has been the maintenance of diode vacuum integrity in the hot gas environment associated with hydrocarbon combustion. This problem is aggravated by the high temperatures associated with hydrocarbon thermionic conversion (1400°C emitter temperature), since gas permeation increases exponentially with temperature. Another major problem area is the development of an efficient regenerative burner at thermionic temperatures, particularly for nongaseous hydrocarbons, to increase generator thermal efficiency.

Isotope thermionic generators would be heavier, bulkier, and less mobile, relative to hydrocarbon systems, largely due to the substantial amount of biological shielding required. However, such units should be capable of longer term, unattended operation due to the long periods between fuelings associated with isotope heat sources such as Sr-90 and Co-60 with their half-lives of 27.7 and 5.25 yr, respectively. In addition, such units could be effectively utilized for undersea applications.

### Isotope Selection

Thermionic devices require a high emitter temperature with a correspondingly high-thermal-flux requirement (20–60 w/cm$^2$). Thus a high-power-density fuel is desired, and only

Presented as Paper 66-1007 at the AIAA Third Annual Meeting, Boston, Mass., November 29–December 2, 1966; submitted December 6, 1966; revision received April 6, 1967. [5.02, 5.08]

* Senior Engineer.

† Manager, Isotopic Power and Radiation Applications Section.

**Table 1 Isotopic power fuels data**

| Radioisotopes | $^{90}$Sr-Y ✓ | $^{137}$Cs-Ba ✓ | $^{147}$Pm | $^{144}$Ce-Pr ✓ | $^{238}$Pu | $^{242}$Cm | $^{244}$Cm | $^{60}$Co ✓ | $^{210}$Po |
|---|---|---|---|---|---|---|---|---|---|
| Half-life, yr | 27.7 | 30 | 2.62 | 0.78 | 87.6 | 0.56 | 18.4 | 5.24 | 0.38 |
| Radiation type[a] | $\beta,\gamma$ | $\beta,\gamma$ | $\beta,\gamma$ | $\beta,\gamma$ | $\alpha,n,\gamma$ | $\alpha,n,\gamma$ | $\alpha,n,\gamma$ | $\beta,\gamma$ | $\alpha,n,\gamma$ |
| Radiation energy, curies/$w_t$ | 148 | 207 | 2790 | 126 | 29.1 | 28 | 29 | 65 | 31.2 |
| Shield thickness[b] | 8 | 5.8 | 1.6 | 15 | (nil) | 10[l] | 3.5 (34)[l] | 13 | 1.4 |
| Typical product form | $SrTiO_3$ | Glass | $Pm_2O_3$ | $CeO_2$ | $PuO_2$ | $Cm_2O_3$-matrix | $Cm_2O_3$ | Metal | Metal |
| Density, g/cm[c] | 3.7 | 3.1 | 6.6 | 6.3 | 9 | 9 | 9 | 8.7 | 9.3 |
| Power, $w_t$/cm$^3$ | 0.82 | 0.24 | 1.8 | 21.9 | 3.6 | 150 | 22.5 | 27[k] 54[k] | 1150 |
| Availability, $kw_t$/yr | | | | | | | | | |
| 1967[d] | 9.5 | 3 | 1 | 4 | 11 | See [i] | See [i] | 130 | 12 |
| 1970[d] | 170 | 140 | 7.2 | 1200 | 15[h] | ... | ... | ... | ... |
| 1980[e] | 770 | 760 | 33 | 7000 | 60 | ... | ... | ... | ... |
| Present AEC price \$/$w_t$[f] | 29.60 | 25.80 | 556 | 18.90 | ... | ... | ... | 32.50 | 780 |
| Future estimated cost \$/$w_t$[g] | 19 | 21 | 93 | 0.90 | 535 | ... | 480 | 10 | 10 |

[a] The symbol $\gamma$ includes bremsstrahlung as well as gamma radiation.
[b] Shield thickness in cm of uranium to reduce a 1000-$w_t$ source to 10 mrad/hr at 1 m.
[c] Power density of the fuel form.
[d] Availability from Atomic Energy Commission (AEC) produced products.
[e] Based on civilian nuclear power operations or special radioisotope production reactors.
[f] Based on large orders and does not include conversion, encapsulation, or shipping costs.
[g] Based on studies assuming large-scale production of encapsulated products.
[h] Could be increased.
[i] Operation now on a developmental basis with cost at 10 $kw_{thermal}$/yr capacity estimated at about \$100/$w_t$.
[j] Operation now on a developmental basis with cost at 5 $kw_{thermal}$/yr estimated at about \$1110/$w_{thermal}$. Production in the range of 100 kw in 1972 and 400 kw in 1980, estimated at a cost of \$480/$w_{thermal}$.
[k] Based on 200 curies/g and 400 curies/g material, respectively.
[l] Cm of $H_2O$ for neutron shielding.

a relatively small area must be thermally insulated in order to obtain the high emitter flux required. Since thermal losses are approximately proportional to insulation area (curves and discontinuities make the exact relationship more complex), the smaller the heat source the less the thermal losses. Since insulation of surfaces at temperatures in the order of 1400°C is critical, a high-power-density fuel is desirable and often mandatory in the design of isotopic thermionic systems.

Another constraint is isotope cost, since for almost every conceivable terrestrial application, an alternate power supply scheme, e.g., batteries or propane thermoelectric generators, can be utilized. The energy cost in \$/kw-hr for isotope generators must, therefore, be competitive. It should be noted that fuel is ordinarily the predominant cost factor for isotope generators. Presently only Co-60 and the fission product beta emitters, e.g., Sr-90, Cs-137, and Ce-144, are sufficiently inexpensive to warrant consideration (see Table 1). Of these, Co-60 has by far the highest power density. A low power density leads to very large sources with correspondingly large surface areas to be insulated. A 1000-w Sr-90 source, for example, would lose ~400 w through 0.5 w/cm$^2$ thermal shielding, including edge losses, leading to only a 60% thermal efficiency.

Ce-144 has the lowest potential cost, but its short half-life (0.76 yr) makes its practicality doubtful, and its radiation characteristics require an excessive amount of gamma and bremsstrahlung shielding. Over-all, Co-60 is most promising for terrestrial isotopic thermionic applications.

The weight required to safely shield a 1000-$w_t$, Co-60 heat source is roughly the same as that required for an equivalent Sr-90 source. This is the case despite the approximately 65% extra shield thickness required to shield a Co-60 source compared to an equivalent Sr-90 source. This apparent paradox can be explained by the fact that Co-60 has a power density about 60 times that of Sr-90, leading to a much smaller volume to be shielded. For example, at 10 $kw_t$, 38,000 lb of depleted uranium would be required to shield Sr-90 (50 mrem/hr at 100 cm) vs ~18,000 lb for the Co-60 source. Ce-137 leads to higher shield weights at all practical power levels due to its very low power density and substantial shield thickness requirements.

### Typical Designs

Figure 1 is a schematic drawing of a possible configuration for a 100-$w_e$, Co-60 undersea thermionic generator. A configuration for a land application would look basically the same minus the pressure vessel. The decay heat from the Co-60 heat source (predominantly gamma photons) is absorbed in both the fuel itself and the thick capsule accumulator walls. Over 90% of the photon energy is converted to thermal energy in the capsule and just 1 in. of the W accumulator material. This heat, 965w, is directed toward the diode emitter. (The insulation is a multifoil vacuum type.) The heat then proceeds across the interelectrode gap to the refractory collector. The heat is then rejected to the seawater via the rigid diode support can, through several more layers of multifoil insulation in another vacuum can, through the U-8Mo biological shield, and finally across the pressure vessel walls.

Figure 2 shows how a 160-$w_e$ terrestrial, thermionic-thermoelectric, cascaded system could be designed. In this design the 1090 w of heat are transferred to the cylindrical emitter

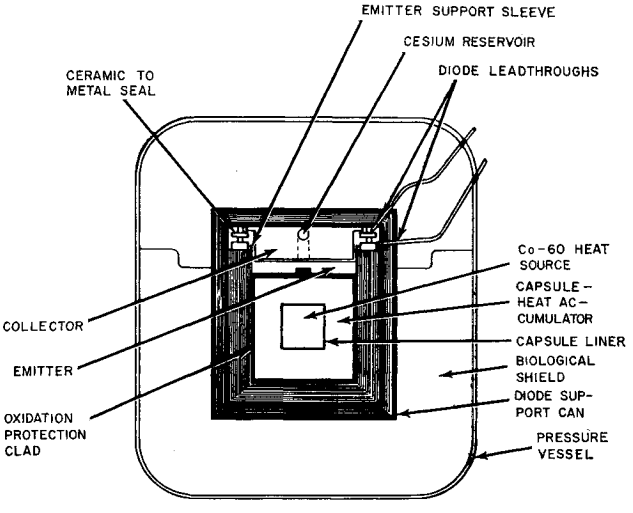


**Fig. 1 Thermionic undersea generator, 100 $w_e$.**

**Table 2 Performance of various 5-yr isotopic SNAP terrestrial generators**

| Unit | SNAP-7D | Advanced thermoelectric | Thermionic, Fig. 1 | Cascaded thermionic-thermoelectric, Fig. 2 |
|---|---|---|---|---|
| Type energy conversion | Lead telluride thermoelectric | Lead telluride bismuth telluride thermoelectric | Cesium diode, gap spacing 8 mils | Lead telluride bismuth telluride T-E + cesium diode |
| Isotope fuel/(w/cm³ fuel) | Sr-90/0.8 | Sr-90/0.8 | Co-60/54 | Co-60/54 |
| Power level, $w_e$ | 60 | 60 | 100 | 160 |
| Hot side temperature | 1000°F | 1100°F | 1400°C | 1400°C/1100°F |
| Data of technology | 1962 | 1965 | 1970 | 1972 |
| Over-all efficiency | 3.8% | 7.0% | 10.8% | 14.7% |
| Total system weight, lb | 4600 | 1100 | 1050 | 950 |
| Over-all size | 22-in. D × 34.5-in. L (except fins) | 28-in. D × 28-in. L (except fins) | 12.5-in. D × 13-in. L | 13-in. D × 17-in. L |
| Energy cost, $/kw-hr | 22.2 | 12.0 | 6.5 | 5.2 |
| Assumed fuel cost, $/$w_{thermal}$ | 19 | 19 | 10 | 10 |

via a lithium heat pipe with a negligible temperature drop. Again the insulation utilized is of the vacuum foil type. A thick sleeve is configured around the exterior of the diode collector to decrease the diode reject heat flux to correspond to a typical PbTe thermopile flux requirement. A segmented lead telluride-bismuth, telluride thermoelectric generator is positioned around the collector outer surface. Since this generator is designed for land application, and heat must now be rejected at the cold junction of the thermopile, cooling fins are required. The cascaded system leads to the highest over-all efficiency now possible with a static low-power system. This results in a less costly, lighter weight, but more complex generator than either a thermoelectric or thermionic generator.

Table 2 compares the foregoing two generators with the SNAP (systems for nuclear auxiliary power)-7D—which is representative of the first generation of isotopic thermoelectric generators and was built by the Martin Company and installed during January 1964, at a Navy boatweather station in the Gulf of Mexico—and an advanced thermoelectric generator based on the use of a high-performance, segmented lead telluride-bismuth telluride thermopile.

## Conclusions

Although the cost and performance potential of thermionic systems are impressive, the following potential problems have been identified which must be resolved, prior to the realization of the performance numbers listed in Table 2:

1) The ability of a Cs diode (and a high-temperature heat pipe if required) to perform reliably for 5 yr has not yet been demonstrated. To date, the longest term continuous operation has been <2 yr. The choice of a relatively low emitter temperature and the trend toward longer lifetimes, however, make such longterm operation in the foreseeable future appear feasible. For many applications, diode replacement every year or two is practical. Only after a more detailed design effort, however, can the practicality of a generator design enabling ease of disassembly and diode replacement in the field be determined.

2) The chosen emitter temperature of 1400°C (and the corresponding 13.5% diode efficiency) represents a marginal operational temperature for the cobalt metal fuel form with its melting point of 1495°C. Either emitter operation at lower temperatures and lower efficiencies or fuel form development might be necessary if it proves impossible to design with only about 100°C $\Delta T$ from emitter to fuel centerline. However, the high conductivity of metallic cobalt (20 Btu/hr-ft-F°) makes design of a low $\Delta T$ system appear feasible.

3) To effectively utilize Co-60 over a 5-yr mission with its 5.25-yr half-life, a mode of thermal-power flattening must be devised. Work has been done in this area and several techniques appear promising.

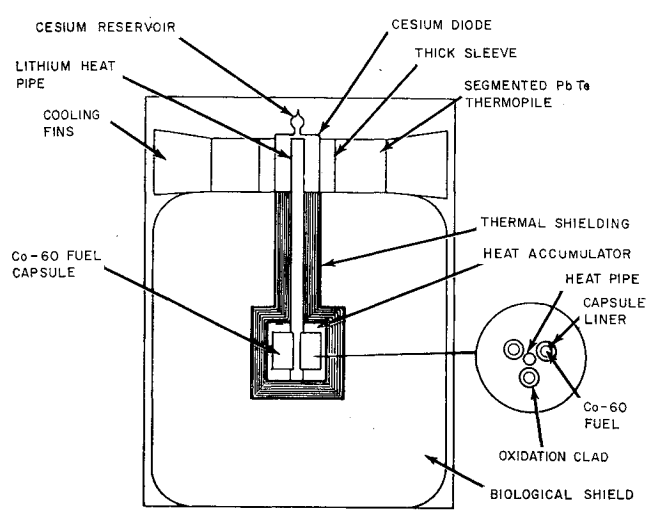


**Fig. 2 Thermionic-thermoelectric cascaded system, 160 $w_e$.**

On the basis of the comparison presented in Table 2, terrestrial thermionic conversion in conjunction with a Co-60 heat source offers substantial performance and cost improvement over thermoelectric SNAP units. Its thermionic thermal match enables the design of efficient compact power supplies in the 60- to 3000-$w_e$ power range. The cascaded thermionic-thermoelectric system, particularly, offers impressive cost and performance characteristics due to the high over-all efficiency associated with thermal cascading. The high over-all efficiency of the thermionic systems, the inherent inexpensiveness of the diode vs a multicouple thermopile, and the low cost of Co-60 fuel lead to these relatively low-cost generators. Any SNAP cost number substantially below 10 would make such units competitive, for many applications, with alternate power supplies such as propane-fired thermoelectric and thermionic generators, air polarized batteries, and lead storage batteries (on a cost comparison basis alone). The mobility, small size and weight, and ability for unattended operation are additional advantages of such SNAP units. Such thermionic generators are particularly advantageous for the host of undersea applications now in the planning stage, since most competitive systems cannot operate in an airless environment.

It is concluded, therefore, that both the Co-60 thermionic and cascaded systems offer sufficient potential to warrant more detailed evaluation. The development problems are indeed substantial, but they are no greater in magnitude than the problems associated with space thermionic development, which is proceeding at a substantial level of effort.

### References

[1] Berkow, H., "Potential requirements for fission product isotopes for power and radiation applications," Hittman Associates, HA-TR-137 (April 17, 1964).

[2] Eastman, G. Y. and Fox, J. A., "Emitter shell materials for fossil fuel fired thermionic converters," *Proceedings of the 19th Annual Power Source Conference*, Power Source Conference Publication Comittee (May 1965).

[3] Walter, J. J., "Radioactive cobalt for heat sources," DuPont Corp., DP-1012 (October 1965).

[4] "Isotope fuels data sheet," Atomic Energy Commission, Division of Isotope Development, Germantown, Md. (April 1966).


# Performance Comparison of Gun-Launched Scramjets for Various Fuels


Nasim F. Amin* and Sannu Mölder†
*McGill University, Montreal, Canada*


THE potential superiority of supersonic combustion ramjet engines (scramjet) for hypersonic atmospheric propulsion (above Mach 7 or so) has been shown by performance[1,2] and trajectory[3] calculations. Since it is an air-breathing engine, with thrust directly related to air mass flow, the scramjet should produce high thrust at high velocities and low altitudes. A gun (16-in. bore, 119 ft long) of the type presently being used by the McGill University/U.S. Army Ballistic Research Laboratory high altitude research project (HARP) on the island of Barbados could launch small scramjets at high velocities at sea level.[3] A previous study of gun-launched, kerosene-fueled scramjets[3] was based on an engine performance program which allowed slight variations in engine geometry during flight and gave no detailed consideration to vehicle weight and volume limitations. The present work is an improvement because the scramjets are of fixed geometry, four fuels are considered, and effects of weight and volume limitations are compared.

Numerous Martlet vehicle firings[4] have demonstrated that aerodynamic vehicles can withstand acceleration loads up to 10,000 $g$'s during gun launch. The writers have investigated some of the structural design problems for scramjets and believe that suitable structures can be developed, but detailed design has not yet been attempted. During launch, the vehicle is supported in the gun barrel by means of either liquid or solid, form-fitting support devices called "sabots." The "shot" weight is the sum of dry vehicle weight, fuel weight, and sabot weight. For all cases considered herein, the dry-vehicle and sabot weights are assumed to be 600 lb and 150 lb, respectively. Gun elevation angles of 90° and 45° represent, typically, a sounding vehicle and a boosting or cruising vehicle, respectively. The charge grain (M8M.225 propellant) size is assumed to be optimized with respect to vehicle weight.[3,4] An increase in shot weight reduces launch velocity but may allow more fuel, so that increase in vehicle weight actually may lead to an increased final velocity and altitude. Thus, the primary problem is volume limitation, with maximum allowable weight being a secondary consideration.

**Table 1 Properties used for four fuels**

| Property | Kerosene | TEA | Shelldyne | Hydrogen |
|---|---|---|---|---|
| Net heating value at 77°F, Btu/lb | 19,200 | 18,352 | 17,886 | 51,571 |
| Density, lb/ft³ | 50 | 52 | 68 | 4.36 |
| Specific heat at 77°F, Btu/lb-°R | 0.47 | 0.527 | 0.363 | 3.434 |
| Stoichiometric fuel/air ratio | 0.067 | 0.0787 | 0.074 | 0.0291 |

Received March 21, 1966; revision received April 10, 1967. This work was sponsored by the Defence Research Board of Canada under Grant 9550-06. [1.01, 4.03, 4.25]


* Research Engineer; now Senior Engineer, Propulsion Section, Los Angeles Division, North American Aviation Inc. Member AIAA.

† Associate Professor of Mechanical Engineering. Member AIAA.


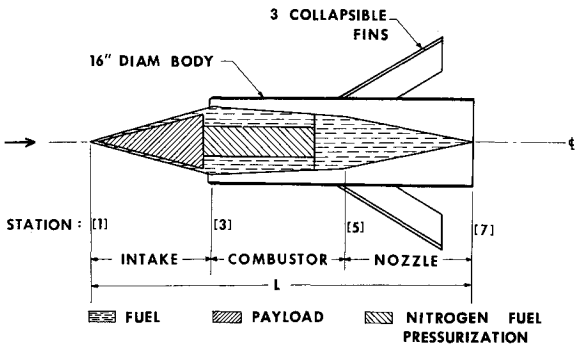


**Fig. 1 Schematic of gun-launched scramjet.**

The fuels compared are kerosene, Shelldyne, triethyl aluminum [TEA, $(C_2H_5)_3Al$], and hydrogen (Table 1). No attempt is made to optimize either the engine or gun performance.

Kerosene has obvious logistic advantages, but it has relatively low reactivity, low cooling capacity, and high-spontaneous ignition temperature (960°R). Shelldyne is a high-density hydrocarbon fuel developed by Shell International Petroleum Co. Ltd., London, for aviation use. It has a low freezing point (448°R) and is storable and safe, but at present it is quite expensive ($45/U.S. gal for laboratory use). Its spontaneous ignition temperature is 906°R. TEA is highly reactive (ignites with air at room temperature and reacts explosively with water), therefore more certain to burn at marginal engine conditions, but difficult to handle; it is usually stored under a slight nitrogen pressure. Liquid hydrogen has the highest heating value per unit mass and high cooling capacity but very low density. In spite of its cryogenic storage problem (36°R), it is expected to be the best fuel for future hypersonic aircraft applications, but it is unlikely to find use in volume-limited applications. Its spontaneous ignition temperature is 1500°R.

### Performance Calculations

Figure 1 shows schematically the vehicle configuration considered. The three fins are spring-loaded and fold into the body while in the gun. Of the 600-lb dry vehicle weight assumed, approximately 200 lb would be useful payload. One-dimensional performance parameters (Table 2) are used throughout the engine,[8] assuming a real gas in chemical equilibrium everywhere, except in the air in the inlet, where only caloric imperfections[7] are considered. An engine cycle analysis program[5] (based on an equilibrium combustion program from the U.S. Naval Ordnance Test Station[6]) has been used to generate Mollier data in the format required by our trajectory performance program.[8] All calculations are for stoichiometric fuel/air mixtures.

The intake defined in Table 2 corresponds approximately to the performance of a two-oblique-shock inlet. Internal skin friction is neglected. The combustor area ratio, $A_5/A_3 = 3.5$, was selected after considerable trial and error; it allows sufficient heat addition at low $M_1$ while still giving good engine performance at high $M_1$. For hydrogen, the vaporized fuel is assumed to be choked at the injector. There is no loss of total enthalpy in the combustion chamber. Combustion and nozzle efficiencies are assumed to be 100%. (These